Polyclonal rabbit antibodies were obtained after three or four immunizations with both *E. coli*– and baculovirus-expressed DmORC2. These polyclonal antibodies were affinity-purified (*21*) by incubation with baculovirus-produced DmORC2 protein coupled to Reactigel beads (Pierce). The eluted antibodies were bound to protein A–Sepharose (Pharmacia) and chemically cross-linked to this support with dimethylpimelimidate (*21*). For immunoprecipitation, 1 μl of these beads was added directly to the respective chromatographic or glycerol gradient fraction, adjusted to 100 mM KCl, incubated for 2 hours at 4°C, and washed six times with 0.1 M KCl–HEMG [25 mM Hepes (pH 7.6), 0.5 mM EDTA, 12.5 mM $MgCl_2$, and 10% glycerol] (*14*). The recovered material was resuspended directly in SDS sample buffer and analyzed by SDS-PAGE.

13. U. Heberlein and R. Tjian, *Nature* **331**, 410 (1988).
14. *Drosophila* Genome Center, Lawrence Berkeley Laboratory, Berkeley, CA; GenBank accession number L39626.
15. E. V. Koonin, *Nucleic Acids Res.* **21**, 2541 (1993).
16. S. K. Hansen, D. T. S. Pak, M. Gossen, S. Zhou, M. R. Botchan, unpublished data.
17. A. E. Ehrenhofer-Murray, M. Gossen, D. T. S. Pak, M. R. Botchan, J. Rine, *Science* **270**, 1671 (1995).
18. V. E. Foe, G. M. Odell, B. A. Edgar, in *The Development of* Drosophila melanogaster, M. Bate and A. M. Arias, Eds. (Cold Spring Harbor Laboratory Press, Cold Spring Harbor, NY, 1993), vol. 1, pp. 149–300.
19. A. B. Blumenthal, H. J. Kriegstein, D. S. Hogness, *Cold Spring Harbor Symp. Quant. Biol.* **38**, 205 (1974); S. L. McKnight and O. L. Miller, *Cell* **12**, 795 (1977); V. A. Zakian, *J. Mol. Biol.* **108**, 305 (1976).
20. R. T. Kamakaka, P. D. Kaufman, B. Stillman, P. G. Mitsis, J. T. Kadonaga, *Mol. Cell. Biol.* **14**, 5114 (1994); C. S. Chiang, P. G. Mitsis, I. R. Lehman, *Proc. Natl. Acad. Sci. U.S.A.* **90**, 9105 (1993).
21. E. Harlow and D. Lane, Eds., *Antibodies* (Cold Spring Harbor Laboratory, Cold Spring Harbor, NY, 1988).
22. Alignments were performed with the ClustalW program [J. D. Thompson, D. G. Higgins, T. J. Gibson, *Nucleic Acids Res.* **22**, 4673 (1994)].
23. Fraction number variation among different glycerol gradients (23 fractions for the molecular mass standards, 20 fractions for recombinant DmORC2, and 21 fractions for the complex) was corrected by normalization of each fraction to V/V_t (the ratio of cumulative eluted volume to total gradient volume). The leftmost and rightmost lanes of each protein immunoblot and silver stain correspond to fractions eluted at 36% and 79% of the total volume, respectively.
24. We thank C. Zuker for providing the *DmORC2* genomic clone, D. Rio for bringing the initial finding of the Zuker lab to our attention, M. Levine (University of California, San Diego) for the plasmid cDNA library, T. Kornberg for the λgt10 cDNA library, D. Rio and R. Tjian for encouragement and technical advice, and A. Ho for help. Supported by a pilot project grant from the National Institute of Environmental Health Sciences Mutagenesis Center (ES-01896), National Cancer Institute grant CA30490, and a Human Frontier Science Program Long-Term Research Fellowship (M.G.). Sequences of the *DmORC2* and *DmORC5* cDNAs have been deposited in GenBank (accession numbers pending).

6 October 1995; accepted 13 November 1995

Early-Onset Epilepsy and Postnatal Lethality Associated with an Editing-Deficient *GluR-B* Allele in Mice

Rossella Brusa, Frank Zimmermann, Duk-Su Koh, Dirk Feldmeyer, Peter Gass, Peter H. Seeburg, Rolf Sprengel

The arginine residue at position 586 of the GluR-B subunit renders heteromeric α-amino-3-hydroxy-5-methyl-4-isoxazolepropionate (AMPA)–sensitive glutamate receptor channels impermeable to calcium. The codon for this arginine is introduced at the precursor messenger RNA (pre-mRNA) stage by site-selective adenosine editing of a glutamine codon. Heterozygous mice engineered by gene targeting to harbor an editing-incompetent *GluR-B* allele synthesized unedited GluR-B subunits and, in principal neurons and interneurons, expressed AMPA receptors with increased calcium permeability. These mice developed seizures and died by 3 weeks of age, showing that GluR-B pre-mRNA editing is essential for brain function.

Glutamate receptors sensitive to AMPA are ligand-activated cation channels that mediate the fast component of excitatory postsynaptic currents in central neurons (*1*). These channels are assembled from four related subunits (GluR-A to GluR-D, or GluR1 to GluR4) (*2*), with the GluR-B subunit rendering the channel almost impermeable to Ca^{2+} (*3*). The molecular determinant for this dominant property of GluR-B was traced to the arginine (R) residue at position 586 of the mature subunit, which lies within the pore-forming segment M2 (*4*). This arginine is not gene encoded (*5*) but is posttranscriptionally introduced into GluR-B pre-mRNA (*5*, *6*) by site-selective adenosine deamination, which leads to the change of a CAA glutamine (Q) codon to a CIG codon for arginine in >99% of mRNA molecules (*5*–*7*). Termed Q/R site editing, this nuclear process depends on a double-stranded RNA structure (*6*) formed in the pre-mRNA by the editing site in exon 11 and the editing site complementary sequence (ECS) in intron 11 (*8*). To investigate in an animal model the relevance of this process for central nervous system (CNS) physiology, we targeted intron 11 of the *GluR-B* gene in mouse embryonic stem (ES) cells (*9*) for replacement of the ECS element (*10*) by *loxP* (*11*, *12*) (Fig. 1), and then injected correctly engineered cells into C57BL/6 blastocysts. One of several resultant chimeric animals showed vertical transmission of the *GluR-B*$^{\Delta ECS}$ allele in a Mendelian fashion (*10*), indicating that the allele did not adversely affect embryonic development.

In brains of *GluR-B*$^{+/\Delta ECS}$ mice, the *GluR-B*$^{\Delta ECS}$ allele was expressed with its transcripts remaining unedited at the Q/R site, demonstrated by analysis of allele-specific reverse transcription–polymerase chain reaction (RT-PCR) products (*13*) of partially spliced GluR-B pre-mRNA (Fig. 2A). The sequence and hybridization analysis of RT-PCR products revealed that pre-mRNA derived from the wild-type allele was edited to the expected extent of 83% (*6*, *13*), whereas pre-mRNA from the *GluR-B*$^{\Delta ECS}$ allele, in which the ECS element was replaced by *loxP*, was not edited at the Q/R site. These data showed that the ECS element is indispensable for Q/R site editing in vivo, as previously established for in vitro editing (*6*, *7*). The RT-PCR analysis further indicated that *GluR-B*$^{\Delta ECS}$ pre-mRNA sequences were amplified more efficiently than *GluR-B*$^{+}$ pre-mRNA (Fig. 2A). Quantification with primers that amplify DNA fragments of identical size for both allelic pre-mRNAs (*13*) revealed that premature transcripts of the *GluR-B*$^{\Delta ECS}$ allele are enriched approximately fivefold in the nucleus as compared with premature transcripts of the *GluR-B*$^{+}$ allele. The nuclear accumulation of *GluR-B*$^{\Delta ECS}$ pre-mRNA was attributable to a reduced splicing efficiency of the sequence-modified intron 11, because ribonuclease (RNase) protection with a suitable intron probe (*14*) revealed increased amounts of the *loxP*-containing intron 11 relative to the unmodified intron (Fig. 2B). Consequently, the amounts of cytoplasmic mRNA corresponding to the two alleles were imbalanced, with mature cytoplasmic transcripts unedited at the Q/R site constituting only 25 ± 3% (mean ± SEM, $n = 8$), rather than the theoretically expected 50%, of the GluR-B mRNA population. This situation reflects an overall decrease in GluR-B mRNA abundance, and, indeed, a reduction of ~30% in the amount of GluR-B mRNA was demonstrated by densitometric analysis of Northern

R. Brusa, F. Zimmermann, P. H. Seeburg, R. Sprengel, Laboratory of Molecular Neuroendocrinology, Center for Molecular Biology (ZMBH), University of Heidelberg, Im Neuenheimer Feld 282, D-69120 Heidelberg, Germany.
D.-S. Koh, D. Feldmeyer, B. Sakmann, Max-Planck-Institut für Medizinische Forschung, Abteilung Zellphysiologie, Jahnstrasse 29, D-69120 Heidelberg, Germany.
P. Gass, Institut für Neuropathologie, University of Heidelberg, Im Neuenheimer Feld 220, D-69120 Heidelberg, Germany.

(RNA) blots (*15*) (Fig. 2C). Other than the imbalance in the mRNAs corresponding to the two alleles, *GluR-B* gene expression appeared normal by Northern analysis, RT-PCR, and in situ hybridization (Fig. 2D). The mutant mRNA was characterized (*13*) by the same flip-flop splice ratios (*16*) and extent of R/G site editing (*17*) as were wild-type transcripts, and the distribution of GluR-B mRNA in the brain was as expected (*18*). In summary, the abundance of GluR-B mRNA in *GluR-B*$^{+/\Delta ECS}$ mice is 70% of that in their wild-type littermates, and one-quarter of these transcripts are unedited at the Q/R site.

In *GluR-B*$^{+/\Delta ECS}$ mice, the functional hemizygosity with regard to Q/R site editing would be expected to result in a shortage of the edited GluR-B subunit for assembly of heteromeric AMPA receptors and, hence, an increase in the glutamate-activated Ca^{2+} permeability of and Ca^{2+} influx through these channels (*19*, *20*). This prediction was confirmed by measurement of responses to fast application of glutamate in nucleated patches isolated from the soma of different neuronal cell types in various brain regions (*21*). For example, in hippocampal pyramidal neurons of the CA1 subfield, the shift of the current reversal potential in a solution containing a high (30 mM) Ca^{2+} concentration to less negative potentials demonstrated that the Ca^{2+} permeability of AMPA receptors in *GluR-B*$^{+/\Delta ECS}$ heterozygotes was 7.3 times that in wild-type homozygotes (Fig. 3). In two other types of principal neurons, cerebellar Purkinje cells and neocortical pyramidal cells, the Ca^{2+} permeability of AMPA receptors in *GluR-B*$^{+/\Delta ECS}$ mice was also increased by a factor of 5.2 to 7.3 (Fig. 3B). Inhibitory basket cells of the dentate gyrus (DG) in *GluR-B*$^{+/+}$ mice showed an average Ca^{2+}/Cs^{+} permeability ratio of 1.2, which is somewhat smaller than that previously estimated from outside-out patch recordings (*22*). This difference is probably attributable to the presence of two classes of basket cells, one of which expresses AMPA receptors with a low Ca^{2+} permeability that give rise to only small ensemble currents (Fig. 3B). These currents could be detected in nucleated patches but not in smaller outside-out patches. Basket cells with lower and higher AMPA receptor–mediated Ca^{2+} permeability occurred also in *GluR-B*$^{+/\Delta ECS}$ mice, in which both groups of cells showed increased Ca^{2+} permeabilities. The difference between the two groups was, however, less pronounced than in *GluR-B*$^{+/+}$ animals (Fig. 3B). Thus, if GluR-B expression is low, as in one class of DG basket cells, the Q/R site–edited subunit would contribute relatively little to the Ca^{2+} permeability of AMPA receptors, and, on average, the increased permeability in the heterozygotes was therefore not as pronounced.

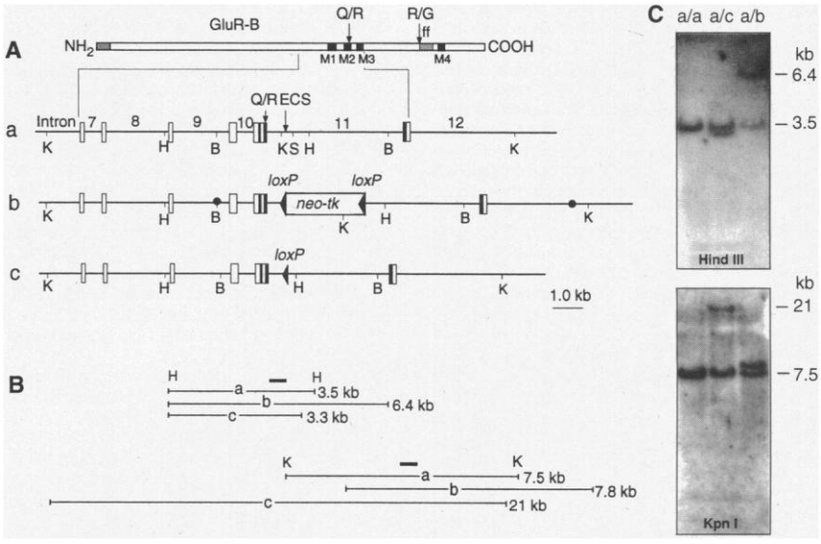

Fig. 1. Generation of *GluR-B*$^{+/\Delta ECS}$ mice. (**A**) Schematic representation of the GluR-B subunit and of gene segments (*8*) of the wild-type *GluR-B*$^{+}$ allele (a), the targeted *GluR-B*^{neo} allele (b), and the *GluR-B*$^{\Delta ECS}$ allele after Cre recombination (c) (*10*). For the protein, Q/R and R/G editing sites (*5*, *6*, *17*) are indicated by arrows; black boxes represent putative membrane segments M1 to M4 (*2*); the hatched box shows the position of the alternatively spliced flip-flop exons (ff) (*16*); and the gray box represents the signal peptide. For the gene segments, open boxes represent exonic sequences (*8*). The *loxP* sites are shown by triangles and the *neo-tk* cassette by an open box. The solid circles in segment b delineate the 5′ and 3′ ends of the targeting construct. Relevant restriction enzyme recognition sites are indicated: K, Kpn I; B, BsrG I; S, Sca I; H, Hind III. (**B** and **C**) Genomic Hind III (H) and Kpn I (K) restriction fragments (B) used in Southern blot analysis (C) to distinguish the *GluR-B* alleles a, b, and c in targeted R1 ES cell clones. Southern probes and their positions (*10*) are indicated by black bars in (B).

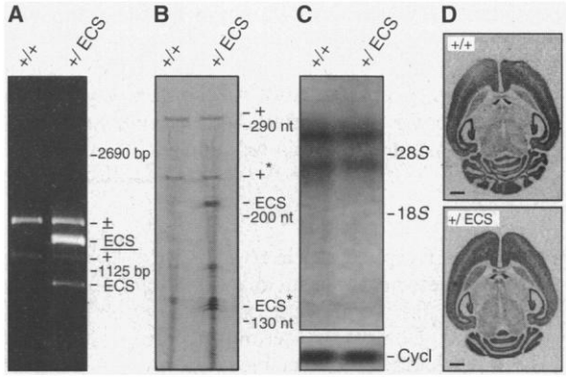

Fig. 2. GluR-B transcript analysis. RNA from the brains of *GluR-B*$^{+/+}$ and *GluR-B*$^{+/\Delta ECS}$ mice was analyzed by various techniques. (**A**) RT-PCR analysis with exon-10 and intron-11 primers (*13*). Amplified fragments containing intron 10 and derived from pre-mRNA or gene sequences are indicated according to allele type by underlined symbols. Amplicons lacking intron 10 and derived from pre-mRNA are denoted by allele symbols that are not underlined, and were cloned for analysis of pre-mRNA. (**B**) RNase protection analysis (*14*). Probe segments protected by the intron-11 sequence in the pre-mRNAs derived from *GluR-B*$^{+}$ and *GluR-B*$^{\Delta ECS}$ alleles are indicated by allele symbols (+, ΔECS). An asterisk indicates probe segments identified as degradation products resulting from overdigestion. Self-protected probe fragments with lower signal intensity are not indicated. (**C**) Northern blot analysis (*15*) with the RNA load controlled for by reprobing the membrane with a probe for cyclophilin mRNA (Cycl). The positions of 28*S* and 18*S* ribosomal RNAs are indicated. (**D**) In situ hybridization of GluR-B mRNA from brains of *GluR-B*$^{+/+}$ (upper panel) and *GluR-B*$^{+/\Delta ECS}$ (lower panel) mice (*18*). Scale bar, 1 mm.

Molecular differences between the *GluR-B*$^{+/+}$ and *GluR-B*$^{+/\Delta ECS}$ animals were revealed in the expression of the Ca^{2+}-responsive immediate-early genes c-*Fos*, c-*Jun*, and *Krox24* (*23*), which likely result from the increased glutamate-activated Ca^{2+} entry into the neurons of heterozygous animals. As observed by in situ hybridization, the abundance of c-*Jun* and *Krox24* (*24*) mRNAs was consistently increased in several brain areas of *GluR-B*$^{+/\Delta ECS}$ mice (Fig. 4A). In particular, c-*Jun* expression was increased in CA1 pyramidal neurons, whereas *Krox24* expression was increased in CA3 pyramidal neurons. Changes in c-*Fos* expression differed among individual heterozygotes, perhaps reflecting the occurrence of spontaneous seizures (see below). In contrast, the abundance of transcripts for AMPA and *N*-methyl-D-aspartate receptor

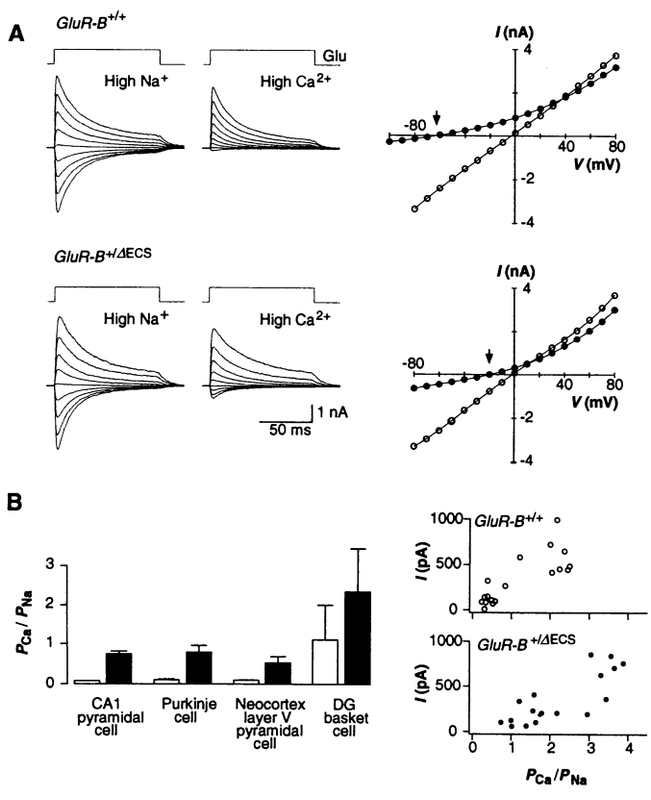

Fig. 3. Relative Ca^{2+} permeability of AMPA receptors in neurons of *GluR-B*$^{+/+}$ and *GluR-B*$^{+/\Delta ECS}$ mice. (**A**) Left panels: AMPA receptor–mediated currents in hippocampal CA1 pyramidal cells evoked by 100-ms pulses of 1 mM glutamate in high-Na^+ and high-Ca^{2+} extracellular solutions, as indicated. The membrane potential was varied between −80 and 80 mV in 20-mV steps. Right panels: Corresponding peak current-voltage (*I-V*) relations for high-Na^+ (○) and high-Ca^{2+} (●) solutions. Arrows indicate the reversal potential in high-Ca^{2+} solution. The *I-V* relations were fitted by third- to sixth-order polynomials, from which the interpolated reversal potentials were calculated. (**B**) Left panel: Ca^{2+} permeability of AMPA receptors in four classes of neurons in *GluR-B*$^{+/+}$ and *GluR*-B$^{+/\Delta ECS}$ mice. Relative Ca^{2+} permeability, expressed as the ratio of Ca^{2+} permeability to Na^+ permeability (P_{Ca}/P_{Na}), is plotted for *GluR-B*$^{+/+}$ (open columns) and *GluR-B*$^{+/\Delta ECS}$ (filled columns) mice. Values are means ± SD of 27 experiments with eight *GluR-B*$^{+/+}$ mice and 46 experiments with seven *GluR-B*$^{+/\Delta ECS}$ mice. Right panels: Plots of relative Ca^{2+} permeability against peak current size at −40 mV in DG basket cells of *GluR-B*$^{+/+}$ and *GluR-B*$^{+/\Delta ECS}$ mice as indicated.

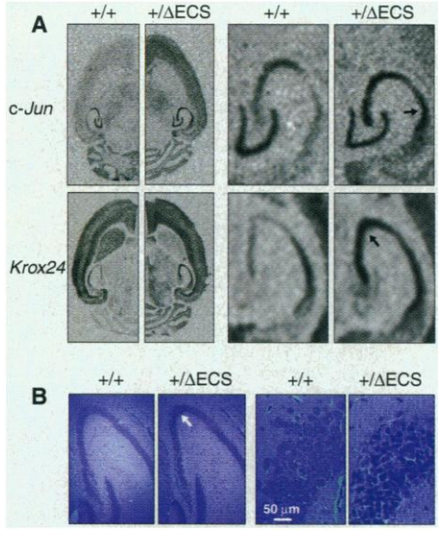

Fig. 4. Histological analysis of brains from *GluR-B*$^{+/+}$ and *GluR-B*$^{+/\Delta ECS}$ mice. (**A**) Autoradiograms of horizontal brain sections (P15) hybridized with ^{35}S-labeled oligonucleotides specific for c-*Jun* and *Krox24* mRNAs (*24*). Half-brain images from wild-type (+/+) and heterozygous (+/ΔECS) mice were apposed to permit better evaluation of expression differences. The hippocampal regions are shown enlarged on the right. Arrows point to the CA3 field for *Krox24* and to the CA1 field for c-*Jun*. (**B**) Hippocampal sections from mouse brains (15 μm), fixed by immersion in 4% paraformaldehyde and embedded in paraffin, were stained with hematoxylin-eosin. The close-ups on the right show the CA3 layer and reveal an increased abundance of eosinophilic cells in the *GluR-B*$^{+/\Delta ECS}$ brain. Arrow indicates the CA3 field.

subunits appeared unaltered (*2*, *16*, *25*).

During the first two postnatal weeks, the heterozygous animals appeared healthy except for an incipient hypotrophy. Beginning at postnatal day 13 (P13), all carriers of the *GluR-B*$^{\Delta ECS}$ allele rapidly developed a severely compromised phenotype, resulting from a neurological syndrome of which the most recognizable manifestations were spontaneous and recurrent seizures, as well as progressively agitated states with excessive jumping and running fits (*26*). All heterozygotes died by P20. Postmortem analysis of the brains of three animals that underwent prolonged seizure episodes revealed selective neuronal degeneration in the lateral region of the hippocampal CA3 field, with ~50% of the neurons showing shrunken nuclei and acidophilic cytoplasmic staining (*27*) (Fig. 4B). Neuronal degeneration was acute in the absence of glial reactions, as assessed by histology and by immunocytochemistry for glial acidic fibrillary protein. Detailed analyses revealed no other apparent abnormalities in the central or peripheral nervous system, and skeletal muscles and visceral organs showed normal histology (*27*). Thus, aberrant excitatory signaling, rather than morphological changes, may underlie the compromised phenotype.

The dominant lethal effect of the *GluR-B*$^{\Delta ECS}$ allele with a penetrance of 100% demonstrates that efficient Q/R site editing of GluR-B pre-mRNA (*5*, *16*) and the resulting low Ca^{2+} permeability of AMPA receptors in excitatory principal neurons (*19*) are pivotal for CNS physiology. Our data suggest that the onset and severity of the epileptic phenotype engendered by a reduction of Q/R site editing depend on the ratio of edited to unedited GluR-B subunits (*28*). It is possible that epileptic mouse models related to altered AMPA receptor properties could be established by regulating this ratio. Indeed, the selective destruction of hippocampal neurons in *GluR-B*$^{+/\Delta ECS}$ mice is reminiscent of kainate-induced hippocampal lesions, which are relevant to human temporal lobe epilepsy (*29*). It remains to be determined whether any of the human familial epilepsies (*30*) derive from related molecular defects.

REFERENCES AND NOTES

1. M. L. Mayer and G. L. Westbrook, *J. Physiol. (London)* **394**, 501 (1987); S. Hestrin, *Neuron* **11**, 1083 (1993); P. Jonas and N. Spruston, *Curr. Opin. Neurobiol.* **4**, 366 (1994).
2. M. Hollmann and S. Heinemann, *Annu. Rev. Neurosci.* **17**, 31 (1994).
3. M. Hollmann, M. Hartley, S. Heinemann, *Science* **252**, 852 (1991); T. A. Verdoorn, N. Burnashev, H. Monyer, P. H. Seeburg, B. Sakmann, *ibid.*, p. 1715.
4. R. I. Hume, R. Dingledine, S. F. Heinemann, *ibid.* **253**, 1028 (1991); N. Burnashev, H. Monyer, P. H. Seeburg, B. Sakmann, *Neuron* **8**, 189 (1992).
5. B. Sommer, M. Köhler, R. Sprengel, P. H. Seeburg, *Cell* **67**, 11 (1991).
6. M. Higuchi *et al.*, *ibid.* **75**, 1361 (1993).
7. T. Melcher, S. Maas, M. Higuchi, W. Keller, P. H. Seeburg, *J. Biol. Chem.* **270**, 8566 (1995); S. M. Rueter, C. M. Burns, S. A. Coode, P. Mookherjee, R. B. Emeson, *Science* **267**, 1491 (1995); J. H. Yang, P. Sklar, R. Axel, T. Maniatis, *Nature* **374**, 77 (1995).
8. M. Köhler, H. C. Kornau, P. H. Seeburg, *J. Biol. Chem.* **269**, 17367 (1994).
9. A. Nagy, J. Rossant, R. Nagy, N. W. Abramow, J. C. Roder, *Proc. Natl. Acad. Sci. U.S.A.* **90**, 8424 (1993).
10. For construction of the targeting vector pGRB-neotk-1, a BsrG I–Sal I mouse 129/sv genomic fragment containing exons 9 to 12 of the *GluR-B* locus (*8*) was subcloned into pBluescript SK II(−) (Stratagene). The 358–base pair (bp) Kpn I–Sca I genomic fragment of intron 11, which contains the ECS site, was deleted and replaced by a *loxP-neo*^{r}*-tk-loxP* cassette from vector pneotk-1 (R. Sprengel, unpublished data). R1 ES cells (*9*) were electroporated (Bio-Rad Gene Pulser set at 240 V and 500 μF) with 40 μg of pGRB-neotk-1 that had been linearized at the unique Sal I site in the polylinker. Cell clones resistant to G418 (300 μg/ml) selection were isolated after 7 to 10 days. Four targeted clones were identified by nested PCR analysis with rsp27 (5′-AGGACGCGCGGGCAAACGAGGGCACCCG-3′) and rsp28 (5′-GCAGGCAAGAGCCGAGGCGAGGCCAAG-3′) as sense primers in intron-9 sequences

outside of the targeting vector and rspneo6 (5′-GCAATCCATCTTGTTCAATGGC-3′) and rsplox5 (5′-CACTGCTCGACCTGCAGCCAAG-3′) as antisense primers of the *neo* cassette. Homologous recombination was confirmed by Southern (DNA) blot analysis (Fig. 1C). To delete the selection marker cassette, 10^7 *GluR-B*$^{+/neo}$ ES cells were electroporated with 30 μg of Cre-encoding plasmid, pMC-Cre (*12*). After 5 to 7 days of ganciclovir (2 μM) selection, the resistant clones were picked and analyzed by PCR with a primer set [sense primer MH53 (5′-GTTGATCATGTGTTTCCCTG-3′) located in intron 11 upstream of the Kpn I site (*6*), and antisense primer rsp36 (5′-CAATAGCAATTGGTGATTTGTGAC-3′) located in intron 11, 3′ of the Sca I site] that amplified a 494-bp fragment of the *GluR-B*$^+$ and a 250-bp fragment of the *GluR-B*$^{\Delta ECS}$ allele. Genotypes of *GluR-B*$^{+/\Delta ECS}$ clones were confirmed on Southern blots (Fig. 1C) of Hind III–digested DNA probed with a 400-bp Bgl II–Kpn I fragment derived from exon-11 and intron-11 sequences, or of Kpn I–digested DNA probed with an 800-bp Bgl II–Hpa I fragment encompassing the 3′ portion of intron 11 and exon 12 (*8*). The absence of *neo* [E. Beck *et al.*, *Gene* **19**, 327 (1982)] and *cre* sequences (*11*) in the genome of the clones was confirmed by PCR. Three independent targeted clones that contained the correct sequence replacement were injected into blastocysts of C57BL/6 mice. Of several male chimeras, only one, derived from clone GRB1/50/Cre/13, transmitted the mutated *GluR-B* allele to offspring, whose genotype was determined from tail DNA by PCR analysis with primers MH53 and rsp36 and by Southern hybridization. Of 89 agouti offspring, 43 were *GluR-B*$^{+/\Delta ECS}$.

11. N. Sternberg, B. Sauer, R. Hoess, K. Abremski, *J. Mol. Biol.* **187**, 197 (1986).
12. H. Gu, Y. R. Zou, K. Rajewsky, *Cell* **73**, 1155 (1993).
13. RT-PCR amplification of GluR-B pre-mRNA sequences from brain tissue [three *GluR-B*$^{+/+}$ animals and six *GluR-B*$^{+/\Delta ECS}$ animals, all P15 to P18] was performed with sense primer rspex10a (5′-GCGGATCCGAATGAGCGTTACGAGGGCTAC-3′, exon 10) and antisense primer rsp36b (5′-CCAATGCATTTGTGACAAATACTGATAATTAAG-3′, intron 11) or, for quantitative studies, MH36 (5′-TCACCAGGGAAACACATGATC-3′, intron 11). For mRNA analysis, amplification primers B52 (*17*) and 3′lamlo [B. Lambolez, E. Audinat, B. Bochet, F. Crepel, J. Rossier, *Neuron* **9**, 247 (1992)], which are derived from exons 11 and 14-15 (*8*), respectively, were used. For analysis of posttranscriptional modifications, the amplicons (Fig. 2A) were directionally cloned into M13mp19 replicative form DNA and recombinant plaques were analyzed by differential oligonucleotide hybridization (*5, 6, 16, 17*) for Q/R site editing in partially spliced pre-mRNA and mRNA, and for ratios of flip-flop splice forms and of R/G site editing in mRNA. Pre-mRNA was analyzed either from RT-PCR products with primers rspex10a and rsp36b, which differ in size for the *GluR-B*$^+$ and *GluR-B*$^{\Delta ECS}$ transcripts and were cloned individually (allele-specific analysis; 17% Q form in *GluR-B*$^+$ pre-mRNA, 100% Q form in *GluR-B*$^{\Delta ECS}$ pre-mRNA), or from RT-PCR products with primers rspex10a and MH36, which are identical in size for the two alleles [17% Q form in *GluR-B*$^{+/+}$ mice; 88 ± 3% (mean ± SD, n = 3) Q form in *GluR-B*$^{+/\Delta ECS}$ mice]. The mRNA analysis (Q forms were assigned to mRNA from the *GluR-B*$^{\Delta ECS}$ allele and R forms to the *GluR-B*$^+$ allele) revealed 25 ± 3% (mean ± SEM, n = 8) Q form in *GluR-B*$^{+/\Delta ECS}$ mice and <1% Q form in *GluR-B*$^{+/+}$ mice; 50 ± 1% (mean ± SD, n = 3) flip in both *GluR-B*$^{\Delta ECS}$ mRNA and *GluR-B*$^+$ mRNA; 71 ± 2% flip R form and 68 ± 5% flop R form in *GluR-B*$^{\Delta ECS}$ mRNA; and 88 ± 2% flip G form and 76 ± 6% flop G form in *GluR-B*$^+$ mRNA.
14. For RNase protection analysis [J. M. Ausubel *et al.*, Eds., *Current Protocols in Molecular Biology* (Wiley Interscience, New York, 1994)], a 315-bp Eco RI–Hinc II fragment from intron 11 of the murine *GluR-B* gene (*8*) was cloned in pBluescript II SK(−). The resulting plasmid was linearized at the Xba I site in the polylinker, and antisense RNA was generated by in vitro transcription with T7 polymerase in the presence of [α-^{33}P]uridine 5′-triphosphate. The ^{33}P-labeled riboprobe [369 nucleotides (nt)] was hybridized to 20 μg of total brain RNA from wild-type and mutant mice and then incubated with RNases A (20 μg/ml) and T1 (1 μg/ml). The major protected RNA fragments were resolved on a 6% polyacrylamide gel and visualized by autoradiography (2 to 6 days of exposure). The sizes of the protected fragments were 316 nt for the *GluR-B*$^+$ and 217 nt for the *GluR-B*$^{\Delta ECS}$ transcripts. Quantification of the protected fragments by densitometric analysis (MacBAS software, Fuji) revealed a three- to fivefold increase in mutant transcripts relative to wild-type transcripts containing intron 11.
15. *GluR-B*–specific signals on Northern blots of brain RNA from *GluR-B*$^{+/\Delta ECS}$ and *GluR-B*$^{+/+}$ animals (P15) obtained with a 350-bp probe (Eco RI, complementary DNA positions 2583 to 2949) derived from the 3′ untranslated region (*8*) were normalized to cyclophilin mRNA [P. E. Danielson *et al.*, *DNA* **7**, 261 (1988)] and quantitatively assessed by densitometry (Fuji Bas 3000). The average relative signal difference between wild-type (n = 2) and heterozygous (n = 10) mice was 30 ± 9% (mean ± SD).
16. B. Sommer *et al.*, *Science* **249**, 1580 (1990).
17. H. Lomeli *et al.*, *ibid.* **266**, 1709 (1994).
18. K. Keinänen *et al.*, *ibid.* **249**, 556 (1990); K. Sakimura *et al.*, *FEBS Lett.* **272**, 73 (1990).
19. P. Jonas, C. Racca, B. Sakmann, P. H. Seeburg, H. Monyer, *Neuron* **12**, 1281 (1994); J. R. P. Geiger *et al.*, *ibid.* **15**, 193 (1995).
20. N. Burnashev, Z. Zhou, E. Neher, B. Sakmann, *J. Physiol. (London)* **485**, 403 (1995).
21. Transverse hippocampal and neocortical slices or parasagittal cerebellar slices with a thickness of 300 μm were cut from the brains of eight *GluR-B*$^{+/+}$ and seven *GluR-B*$^{+/\Delta ECS}$ mice (P14 to P19). Cells were identified visually by infrared differential interference contrast video microscopy [G. J. Stuart, H.-U. Dodt, B. Sakmann, *Pflüegers Arch.* **423**, 511 (1993)]. DG basket cells were also identified by their location at the hilar border of the DG, the triangular shape of their soma, and their discharge pattern (*19*). To increase the size of currents mediated by AMPA receptors, we performed electrophysiological experiments with nucleated patches [W. Sather, S. Dieu- donné, J. F. MacDonald, P. Ascher, *J. Physiol. (London)* **450**, 643 (1992)] that had diameters of 7 to 12 μm. In some experiments with cerebellar Purkinje cells, outside-out patches were used. Slices were continuously superfused with physiological extracellular saline solution, containing 125 mM NaCl, 25 mM $NaHCO_3$, 25 mM glucose, 2.5 mM KCl, 1.25 mM NaH_2PO_4, 2 mM $CaCl_2$, and 1 mM $MgCl_2$, that was bubbled with 95% O_2 and 5% CO_2. A Hepes-buffered high-Na^+ extracellular solution, used for perfusing the application pipette, contained 135 mM NaCl, 5.4 mM KCl, 1.8 mM $CaCl_2$, 1 mM $MgCl_2$, and 5 mM Hepes-NaOH (pH 7.2). The high-Ca^{2+} extracellular solution contained 30 mM $CaCl_2$, 105 mM *N*-methyl-D-glucamine, and 5 mM Hepes-HCl (pH 7.2). D-2-Amino-5-phosphonovaleric acid (25 μM) was added to block *N*-methyl-D-aspartate receptor channels. The high-Cs^+ intracellular solution contained 140 mM CsCl, 10 mM EGTA, 2 mM $MgCl_2$, 2 mM adenosine triphosphate (disodium salt), and 10 mM Hepes-CsOH (pH 7.3). The P_{Ca}/P_{Na} values were determined from the reversal potentials in Na^+-rich extracellular solution (V_{revNa}) and Ca^{2+}-rich extracellular solution (V_{revCa}) according to the following equation:

$$P_{Ca}/P_{Na} = 0.25\, a_{Na}/a_{Ca}\{\exp[(2V_{revCa} - V_{revNa})F/RT] + \exp[(V_{revCa} - V_{revNa})F/RT]\}$$

where a_{Na} and a_{Ca} are the activities of Na^+ and Ca^{2+} in the extracellular solutions, respectively, and R, T, and F have their conventional meaning [C. A. Lewis, *J. Physiol. (London)* **286**, 417 (1979)]. Activity coefficients were estimated by interpolation of tabulated values (0.75 for NaCl, 0.55 for $CaCl_2$). Both V_{revCa} and V_{revNa} values were corrected for liquid junction potentials of 9.8 and 4.5 mV, respectively.
22. D.-S. Koh, J. R. P. Geiger, P. Jonas, B. Sakmann, *J. Physiol. (London)* **485**, 383 (1995).
23. J. I. Morgan and T. Curran, *Annu. Rev. Neurosci.* **14**, 421 (1991); P. Gass, T. Herdegen, R. Bravo, M. Kiessling, *Neuroscience* **48**, 315 (1992); W. J. Gallin and M. E. Greenberg, *Curr. Opin. Neurobiol.* **5**, 367 (1995).
24. W. Wisden *et al.*, *Neuron* **4**, 603 (1990).
25. M. Watanabe, Y. Inoue, K. Sakimura, M. Mishina, *Neuroreport* **3**, 1138 (1992); T. Ishii *et al.*, *J. Biol. Chem.* **268**, 2836 (1993); H. Monyer, N. Burnashev, D. J. Laurie, B. Sakmann, P. H. Seeburg, *Neuron* **12**, 529 (1992).
26. All heterozygotes developed overt behavioral seizures [R. J. Racine, *Electroencephalogr. Clin. Neurophysiol.* **32**, 281 (1972)]. A total of 14 heterozygous and 10 wild-type mice were observed from P12 for various time periods (8 to 12 hours), and representative video recordings were made. At P13 to P14, all heterozygotes, but none of the wild-type mice, developed recurrent seizures with a "behaviogram" similar to that of kainic acid–induced limbic seizures [J. V. Nadler, *Life Sci.* **29**, 2031 (1981)], characterized by rearing on hindlimbs and concomitant forelimb tremor. In addition to these limbic seizure episodes, animals showed spontaneous tonic-clonic seizures (persisting for 20 to 60 s) followed by drowsiness and altered states of consciousness. On average, generalized seizures occurred two to three times during observation periods. These seizures alternated with jumping and running fits over periods of 2 to 3 hours, and persisted for ~2 days. In the subsequent days (P16 to P20), the heterozygous mice developed a severely compromised phenotype characterized by growth retardation, weakness of the hindlimbs, progressively agitated states with chewing-grooming automatisms, excessive jumping and running fits, and, finally, stupor and death.
27. For histological analyses [B. D. Distrey and J. H. Rack, *Histological Laboratory Methods* (E. & S. Publishers, Edinburgh, U.K., 1970)], two heterozygous and two wild-type mice were perfused transcardially with 4% paraformaldehyde at ages P15, P17, P18, and P19. Brain and visceral organs were dissected, embedded in paraffin, and analyzed as 1-μm sections. Apart from hypotrophy of all organ systems, no gross abnormalities were evident in the central or peripheral nervous system, skeletal muscles, or visceral organs of heterozygotes. In the CNS, all major neuronal populations were present and did not show histological abnormalities, as judged by light microscopic examination of serial sections (1-μm coronal sections every 100 μm) treated with Nissl's stain or hematoxylin-eosin. The cortex of the telencephalon and cerebellum exhibited regular layering. Myelination was also equal in mutant and wild-type animals, as assessed by histochemistry (Klüver-Barrera staining) and immunocytochemistry for myelin basic protein. Marker molecules for specific neuronal subpopulations, including tyrosine hydroxylase, glutamate decarboxylase, parvalbumin, and calbindin [K. D. Beck, L. Powell-Braxton, H. R. Widmer, J. Valverde, F. Hefti, *Neuron* **14**, 717 (1995)], showed the same distribution and were detected in similar numbers of neurons in mutant and wild-type animals. Equal numbers of astrocytes expressing glial fibrillary acidic protein were observed in wild-type and mutant mice, and these cells were particularly abundant in the hippocampus and along white matter tracts.
28. Two chimeric founders derived from the targeted cell line containing the *neo* cassette in intron 11 (Fig. 1A, allele b) gave rise to *GluR-B*$^{+/neo}$ offspring. *GluR-B*$^{+/neo}$ mice had a ratio of Q/R site–edited to –unedited GluR-B mRNA of 10:1 (n = 2), and of 14 heterozygotes only 2 died of seizure-related causes around P30.
29. S. Nakajima, J. E. Franck, D. Bilkey, R. A. Schwartzkroin, *Hippocampus* **1**, 67 (1991).
30. W. A. Hauser and D. C. Hesdorffer, *Epilepsy: Frequency, Causes, and Consequences* (Demons, New York, 1990); J. O. McNamara, *J. Neurosci.* **14**, 3413 (1994).
31. We thank B. Sakmann and M. Kiessling for their interest and support; I. Schiller and H. Monyer for critical discussions; M. Higuchi for advice and materials; A. Nagy for the R1 ES cell line; H. Gu for the plasmids pGEM-30, pGH-1, and pMC-Cre; A. Herold for DNA sequencing; U. Amtman for help with in situ hybridization; and R. Pfeffer for animal care. R.B. was the recipient of a doctoral fellowship from the University of Torino, Italy. Supported, in part, by Sonderforschungsbereich grant 317 and funds from the German Chemical Society to P.H.S.

14 September 1995; accepted 24 October 1995